

CALCULATION OF AERODYNAMIC CHARACTERISTICS OF WING AND  
FUSELAGE IN SUPERSONIC FLOW

M. Enselme

GPO PRICE \$ \_\_\_\_\_

CFSTI PRICE(S) \$ \_\_\_\_\_

Hard copy (HC) 1.00Microfiche (MF) 1.50

ff 853 July 85

Translation of "Calcul des caractéristiques aérodynamiques  
d'un ensemble aile-fuselage en écoulement supersonique."  
Paper Presented at the Royal Aeronautical Society Centenary  
Congress in Conjunction with the Fifth Congress of the  
International Council of the Aeronautical Sciences at the  
Royal Garden Hotel, Kensington, London SW 7,  
September 12-16, 1966; ONERA, France.

ICAS Paper No. 66-22

FACILITY FORM 802	<b>N67 13792</b>	
	(ACCESSION NUMBER)	(THRU)
	<u>14</u>	<u>1</u>
	(PAGES)	(CODE)
	(NASA CR OR TMX OR AD NUMBER)	<u>01</u>
		(CATEGORY)

NATIONAL AERONAUTICS AND SPACE ADMINISTRATION  
WASHINGTON NOVEMBER 1966

CALCULATION OF AERODYNAMIC CHARACTERISTICS OF WING AND  
FUSELAGE IN SUPERSONIC FLOW

/1\*\*

M.Enselme\*

A brief review of the supersonic aerodynamics problem of wing-fuselage interaction, to be solved with the lifting surface theory, is followed by a description of the principle of the proposed analog method. A two-dimensional network of inductances and capacitances represents partial derivatives where the analog of time is identified with the spatial variable taken along the velocity, with the aerodynamic boundary conditions transformed into the electric conditions imposed at the network boundaries. For developing a computation method and for checking its velocity, a comparison between analog computer and wind tunnel is given for a delta-wing aircraft at various Mach numbers. The results of the study are presented.

## 1. Introduction

The representation of the boundary conditions, required for calculating the perturbation velocity potential induced by the presence of a wing-fuselage assembly in a supersonic flow, is rather difficult to introduce into digital computation.

Using the method of conical flow (Ref.1), it is rather easy to represent a fuselage in the form of a cone of the same vertex as the wing which is assumed to have a delta configuration. Conversely, the effect of the presence of a cylindrical body which most closely approaches the real shape of the fuselage of a given aircraft, is impossible to calculate.

Also with the method of sources, the solution is difficult to make explicit despite the fact that the basic principle is known: It is sufficient to distribute sources over the fuselage and wing surface and to calculate from this the potential induced on the wing-fuselage assembly; however, from the practical viewpoint this leads to a considerable increase in the time required for computation since the elementary solutions of each individual source depend on the three coordinates  $x$ ,  $y$ ,  $z$ . So far as we know, this problem has never been solved in its entire generality.

Conversely, the method of analog computation, developed for the isolated

---

\* Chief of the Research Division of the ONERA (National Aerospace Research and Development Administration), France.

\*\* Numbers given in the margin indicate pagination in the original foreign text.

wing (Ref.2), can be extended to include the solution of this particular problem, at least in the case of a circular or non-circular cylindrical fuselage, since it has the advantage of representing the space  $ox, oy, oz$  at the interior of which the function  $\varphi$  is defined.

This method of analog computation will be discussed here, after reviewing the aerodynamic conditions of the problem; this is followed by a comparison of the preliminary results of the calculation with experimental data obtained in various wind tunnels on a standard mockup.

## 2. Aerodynamic Problem

/2

Let us consider a wing-fuselage assembly, placed at a certain angle of incidence in a flow of infinite velocity  $U_0$  (Fig.1). The perturbation velocity potential, as in the case of the isolated wing, satisfies the equation

$$\frac{\partial^2 \varphi}{\partial y^2} + \frac{\partial^2 \varphi}{\partial z^2} = (M_0^2 - 1) \frac{\partial^2 \varphi}{\partial x^2}. \quad (1)$$

The boundary conditions on the wing are as follows:

- a)  $\frac{\partial \varphi}{\partial z} = -U_0 \alpha$  on the planform of the wing mapped onto a plane parallel to  $U_0$ ;
- b)  $\varphi(x, y, 0) = 0$  outside of the wing and the wake.

On the fuselage, if  $\vec{n}$  defines the normal, the condition of sideslip leads to satisfaction of the relation

$$\vec{n} \cdot \text{grad} (\varphi + U_0 x) = 0$$

or else

$$\frac{\partial \varphi}{\partial n} = -U_0 (\vec{i} \cdot \vec{n}) \quad (2)$$

where  $\vec{i}$  is a unit vector attached to  $ox$ .

Denoting by  $\alpha' \beta' \gamma'$  the direction cosines of the normal in a trihedron fixed with respect to the fuselage (Fig.1) and by  $i', j', k'$  the unit vectors selected on these axes, we will obtain, noting that  $\vec{i} = \vec{i}' + \alpha k'$  (where  $\alpha$  is the angle of attack),

$$\frac{\partial \varphi}{\partial n} = -U_0 (\alpha' + \alpha \gamma').$$

Assuming that the fuselage is a body of revolution and denoting by  $\theta$

/3

the polar angle relative to a point of the fuselage (for a given value of  $x'$ ), it can be demonstrated that

$$\alpha' = \frac{dr}{ds} \quad \text{and} \quad \gamma' = \frac{dx'}{ds} \sin \theta$$

where  $r(x')$  and  $s$  define, respectively, the meridian and the curvilinear abscissa along this meridian (Fig.1).

Consequently, the condition is written in this case:

$$\frac{\partial \varphi}{\partial n} = -U_0 \left[ \frac{dr}{ds} + \alpha \frac{dx'}{ds} \sin \theta \right]. \quad (3)$$

It should be noted that in the problem of lift discussed in this paper, the first term of the expression of the normal derivative, not contributing to the lift, will be disregarded; this results in

$$\frac{\partial \varphi}{\partial n} = -U_0 \alpha \frac{dx'}{ds} \sin \theta, \quad (4)$$

which, for the cylindrical portion of the fuselage, leads to

$$\frac{\partial \varphi}{\partial n} = -U_0 \alpha \sin \theta. \quad (5)$$

The totality of the boundary conditions, expressed in this manner, is plotted in Fig.2. To simplify the representation, let us consider, in Fig.3, the boundary conditions referring to the flow around the isolated fuselage. Let  $\varphi_1$  be the corresponding potential: on the fuselage assumed to be a body of revolution, we have  $\frac{\partial \varphi_1}{\partial n} = -U_0 \alpha \frac{dx'}{ds} \sin \theta$  and in the plane  $z = 0$ ,  $\varphi = 0$ .

Forming the difference between  $\varphi$  and  $\varphi_1$ , the resultant potential  $\varphi_2$  will satisfy the boundary conditions shown in Fig.4. The normal derivative of this potential is zero on the fuselage whereas, on the wing, it assumes the following value:

$$\frac{\partial \varphi_2}{\partial z} = -U_0 \alpha - \left( \frac{\partial \varphi_1}{\partial z} \right)_{z=0}. \quad (6)$$

If it is assumed that the fuselage is cylindrical at the wing root and if its ogive nose portion is considered to be sufficiently far upstream so as not to disturb the vertical velocity distribution at the level of the wing  $W =$

$= \frac{\partial \varphi_1}{\partial z}$ , then the following expression can be taken on the wing:

$$\frac{\partial \varphi_1}{\partial z} = U_0 \alpha \frac{R^2}{y^2} \quad (7)$$

a value which corresponds to Ward's approximation for a streamlined body.

Thus the normal derivative of the potential  $\varphi_2$  will have the following expression:

$$\frac{\partial \varphi_2}{\partial z} = - U_0 \alpha \left[ 1 + \frac{R^2}{y^2} \right]. \quad (8)$$

Overall, the problem is thus decomposed into two parts:

a) Calculation of the wing-fuselage system, satisfying the following boundary conditions:

$$\frac{\partial \varphi_2}{\partial n} = 0 \quad \text{on the fuselage} \quad (9)$$

$$\frac{\partial \varphi_2}{\partial z} = - U_0 \alpha \left( 1 + \frac{R^2}{y^2} \right) \quad \text{on the wing.} \quad (10)$$

b) Calculation of the isolated fuselage, using for example the theory <sup>15</sup> of slender bodies; in fact, this calculation is reduced to determining the potential distributions over the nose section since the fuselage is assumed to be cylindrical at the wing root.

The sought potential  $\varphi$  is then obtained by performing summation over  $\varphi_2$  and  $\varphi_1$ , noting that  $\varphi$  differs from  $\varphi_2$  only on the fuselage since, on the wing, we have  $\varphi_1 \equiv 0$ .

### 3. The Analog Problem

It had been shown in a previous paper (Ref.2) that it is possible to represent the aerodynamic potential, induced by the presence of a wing in a stationary or nonstationary supersonic flow, by a method of analog computation. Let us recall that this analog method consists in simulating the wave equation of the aerodynamic problem by a two-dimensional network consisting of inductances and capacitances, intersecting the plane  $yo\bar{z}$  perpendicularly to the velocity of flow, with the variable  $x$  being represented by the analog time. The electric boundary conditions are obtained by transposition of the aerodynamic conditions; the sequence of operations to be made on the network are shown schematically in Fig.4.

This computation process can be generalized for studying the wing-fuselage unit; in fact, it is sufficient to represent, in the plane  $zy$  which is perpendicular to the velocity  $U_0$ , the trace of the fuselage and to apply the condition  $\frac{\partial \varphi_2}{\partial n} = 0$  to this contour. Unfortunately, a difficulty appears in changing to

practical realization since the plane  $yoz$  is intersected at a certain number of square meshes and since it is obviously highly improbable that the trace  $C$  of the fuselage will pass through the nodes of this network; even if this were the case, the transposition of the boundary conditions would be very difficult to perform because of the orientation of the strands of the network with respect to the normal to the fuselage surface at the point under consideration.

Consequently, we preferred a conformal mapping, connecting the exterior 16 with the contour  $C$  at the plane  $YOZ$ . In view of the transformation used

$$\eta = \zeta - \frac{R^2}{\bar{\zeta}} \quad (11)$$

where  $\eta = Y + iZ$  and  $\zeta = y + iz$ , the circle  $\zeta = R e^{i\theta}$  corresponds to the two edges of the intercept  $(2iR, -2iR)$  as shown in Fig.5, with  $Z = 2z$  as point correspondence. The axis  $oy$ , exterior to the circle, has the axis  $OY$  as image

with  $Y = y \left(1 - \frac{R^2}{y^2}\right)$  as connection.

Let us now investigate the form assumed by the equation of partial derivatives in the plane  $YOZ$ . Although, in the conventional applications of conformal transformations to harmonic functions, the property of harmonicity is conserved during the transformation, it is obviously necessary here to make allowance for the influence of the modification in length introduced by this correspondence into the expression of the anharmonic equation.

Let us recall the computation process: Since the preservation of angles and of the potential difference between two homologous points is ensured by the conformal mapping, this can be written on the basis of the two relations:

$$d\varphi = \overrightarrow{\text{grad}} \varphi \cdot d\vec{M}$$

$$\text{and } d\varphi' = \overrightarrow{\text{grad}} \varphi' \cdot d\vec{M}'$$

$$\frac{|\overrightarrow{\text{grad}} \varphi|}{|\overrightarrow{\text{grad}} \varphi'|} = \frac{|dM'|}{|dM|}$$

Otherwise, the ratio of the Laplacians of  $\varphi$  and  $\varphi'$  for the variables  $y, z$  and  $Y, Z$  is written as follows:

$$\frac{\Delta \varphi_{yz}}{\Delta \varphi'_{YZ}} = \frac{\text{div}(\overrightarrow{\text{grad}} \varphi)}{\text{div}(\overrightarrow{\text{grad}} \varphi')}$$

However,

$$\text{div}(\overrightarrow{\text{grad}} \varphi) dS = \int \vec{n} \cdot \overrightarrow{\text{grad}} \varphi d\sigma$$

$$\text{div}(\overrightarrow{\text{grad}} \varphi') dS' = \int \vec{n}' \cdot \overrightarrow{\text{grad}} \varphi' d\sigma'$$

17

where  $ds'$  denotes the homolog of the element  $ds$  of the closed curve limiting the area  $dS$ .

This yields

$$\frac{\Delta \varphi_{yz}}{\Delta \varphi'_{yz}} = \frac{|\text{grad } \varphi|}{|\text{grad } \varphi'|} \cdot \frac{ds'}{ds} = \left| \frac{ds'}{ds} \right|^2 = \left| \frac{d\eta}{d\xi} \right|^2.$$

In the case of the relation  $\eta = \zeta - \frac{R^2}{\zeta}$  under consideration, this relation permits writing

$$\Delta \varphi = \Delta \varphi' \cdot \left| 1 + \frac{R^2}{\zeta^2} \right|^2$$

which, in explicitly expressing the equation as a function of the coordinates  $yz$ , becomes

$$\Delta \varphi'_{yz} = \frac{(z^2 + y^2)^2}{(z^2 + y^2)^2 - 2R^2(z^2 - y^2) + R^4} \Delta \varphi_{yz}. \quad (12)$$

Then, according to the expression for  $\Delta \varphi_{yz}$ , it follows that

$$\Delta \varphi'_{yz} = \frac{(z^2 + y^2)(M_0^2 - 1)}{(z^2 + y^2)^2 - 2R^2(z^2 - y^2) + R^4} \frac{\partial^2 \varphi}{\partial x^2}. \quad (13)$$

Let us now discuss the analog transposition of this equation, by assuming the plane  $Y, Z$  as intersected by a network consisting of inductances connecting the contiguous nodes located on parallels to the axes  $OY$  and  $OZ$  and of capacitances  $C$  connecting each node to a common reference potential.

In a manner identical with the process described elsewhere (Ref.2), it can be demonstrated that the electric potential of such a network satisfies the equation

$$\frac{\partial^2 V}{\partial Y^2} + \frac{\partial^2 V}{\partial Z^2} = \frac{L_0 C}{h^2} \frac{\partial^2 V}{\partial t^2} \quad (14)$$

with an accuracy due to the representation of the partial derivatives by finite differences.

So as to obtain analogy between eqs.(14) and (13), it is necessary to assume each capacitance  $C$ , located at the coordinate point  $Y, Z$ , as being proportional to

$$\frac{(z^2 + y^2)^2}{(z^2 + y^2)^2 - 2R^2(z^2 - y^2) + R^4}$$

where  $y, z$  denote the coordinates of the image point of  $Y, Z$ .

Denoting by  $C_0$  the capacitance corresponding to a point at infinity, we will thus obtain

$$\frac{C}{C_0} = \frac{(z^2 + y^2)^2}{(z^2 + y^2)^2 - 2R^2(z^2 - y^2) + R^4} \quad (15)$$

This relation must be supplemented by the expression

$$t = \frac{x\sqrt{L_0 C_0}}{\sqrt{M_0^2 - 1}} \quad (16)$$

defining  $t$  as a function of  $x$ .

Let us now examine the electric conditions to be imposed, as a function of time, to the contour which, because of the symmetry of the problem, is composed of the two semiaxes  $OY$  and  $OZ$ :

a) On the wing, the sideslip condition [eq.(8)]

$$\frac{\partial \varphi_z}{\partial z} = -\alpha \left[ 1 + \frac{R^2}{y^2} \right]$$

is transformed into

$$\left( \frac{\partial \varphi_z'}{\partial z} \right)_{z=0} = \left( \frac{\partial \varphi_z}{\partial z} \right)_{z=0} \cdot \left| \frac{dz}{d\eta} \right|_{z=0} \quad (17)$$

which yields

$$\frac{\partial \varphi_z'}{\partial z} = -\alpha \quad (18)$$

Considering a node of the network located on the wing, as indicated in Fig.6, and denoting by  $I$  the current intensity entering the network through this point, the following relation can be written in accordance with Kirchhoff's law

$$\frac{V_1 - V_0}{L^*} + \frac{V_2 - V_0}{L_0} + \frac{V_3 - V_0}{L^*} + \frac{dI}{dt} = \frac{1}{C^*} \frac{\partial^2 V}{\partial t^2} \quad (19)$$

or else

$$\frac{h^2}{L^*} \frac{\partial^2 V}{\partial y^2} + \frac{h}{L_0} \frac{\partial V}{\partial z} + \frac{h^2}{2L_0} \frac{\partial^2 V}{\partial z^2} + \frac{dI}{dt} = \frac{1}{C^*} \frac{\partial^2 V}{\partial t^2}$$

which demonstrates that, if it is desired to satisfy, at this point, both the equation and the boundary conditions, one must necessarily have

$$L' = 2L, \quad C' = \frac{C}{2} \text{ and } \frac{h}{L_0} \frac{\partial V}{\partial z} = - \frac{dI}{dt}. \quad (20)$$

Combining eqs.(18) and (20), we obtain

/10

$$\frac{dI}{dt} = \frac{h}{L_0} U_0 \alpha \quad (21)$$

a relation that defines the electric current to be applied at each point affected by the wing.

At the exterior of the wing, let us recall that  $V(Y, 0, t) \equiv 0$ .

b) On the fuselage, i.e., along the segment  $0 - 2Ri$ , the normal derivatives in the planes  $oyz$  and  $OYZ$  are interconnected by

$$\frac{\partial \varphi'_2}{\partial y} = \frac{\partial \varphi_2}{\partial n} \left| \frac{\partial \xi}{\partial n} \right|_{\text{for } \xi = R e^{i\theta}}$$

whence

$$\frac{\partial \varphi'_2}{\partial y} = \frac{1}{2 \cos \theta} \cdot \frac{\partial \varphi_2}{\partial n}.$$

In the case of interest here, it has been demonstrated that  $\frac{\partial \varphi_2}{\partial n} = 0$  on the fuselage, so that

$$\frac{\partial \varphi'_2}{\partial y} = 0.$$

The electric network thus will be left free all along the axis  $OZ$ .

#### 4. Electric Realization

The realization requires an electronic unit capable of realizing short-circuits to satisfy the condition  $V = 0$  upstream of the leading edge and for triggering the linear-intensity generators at the exact instant defined by the equation  $t_{1,e}(y)$  imaging the leading edge. This ensemble is identical to that developed for the calculation of the isolated wing. /11

The electric network has a very similar composition except for the fact that the capacitances  $C$  are no longer the same at each point but must be adjusted to the local value defined by eq.(15): A numerical computation permits a preliminary definition of the values at each node of the meshes.

A photograph (Fig.7) of the assembled device, including display of the boundary conditions, circuits, and measuring devices, gives a general idea of the electric connections used.

## 5. Applications

To verify the validity and to evaluate the accuracy of an experimental computation method it is always necessary to compare the obtained results with those furnished by theoretical calculations. In our case, we were able only to compare these results with data obtained in a wind tunnel; however, it was possible to prove, in the particular case of a cylindrical fuselage at an angle of attack, that the analog values agree well with the theoretical data.

For a comparison between analogy and wind tunnel, we used the results of a comprehensive study made in various wind tunnels on a delta wing combined with a cylindrical fuselage. The object of this experimental study was to define, within the scope of the AGARD\* program, a mockup useful as a standard for various supersonic wind tunnels. The geometric characteristics of this wing + fuselage system are shown in Plate 1.

The analog study with respect to this aircraft permitted defining the perturbation potential and thus, specifically, the lift coefficient and the position of the center of pressure; this calculation was repeated for various Mach numbers. A comparison of the overall coefficients is given in Plates 2 and 3 where a satisfactory agreement between wind-tunnel data and analog computation is evident. Plates 4 and 5 give typical examples for the distribution of flow over the wing span and for the loci of the local centers of pressure. /12

## 6. Conclusions

In this paper, we presented the principle of an analog computation method for a combination of wing + cylindrical fuselage in supersonic flow. The preliminary results agree well with the values obtained in the wind tunnel. Other tests on the influence of the position of the wing with respect to the fuselage are in progress and will be discussed in a later publication.

It should be noted that this mode of computation can be extended also to other problems of interaction, different from the one treated here, and specifically to calculations of biplanes, including flying wings, as well as to calculations of the effect of wing dihedral.

## REFERENCES

1. Germain, P.: General Theory of Conical Motion and its Application to Super-

---

\* AGARD = Advisory Group for Aeronautical Research and Development, North Atlantic Treaty Organization.

- sonic Aerodynamics (La théorie générale des mouvements coniques et ses applications à l'aérodynamique supersonique). ONERA Publ. No.34.
2. Enselman, M.: Analog Computation of a Wing in Supersonic Flow (Sur le calcul analogique d'une aile en écoulement supersonique). Compt. Rend., Vol.257, pp.3115 - 3117.

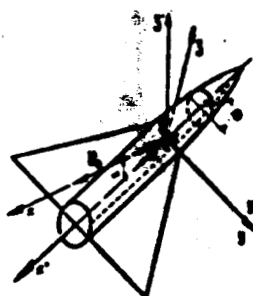


Fig.1 Reference Trihedron of Wing-Fuselage System.

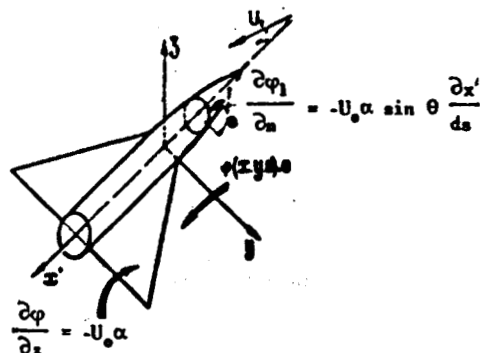


Fig.2 Boundary Conditions, Defining  $\varphi$ .

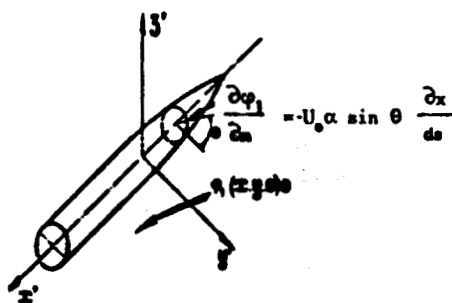


Fig.3 Boundary Conditions, Defining  $\varphi_1$ .

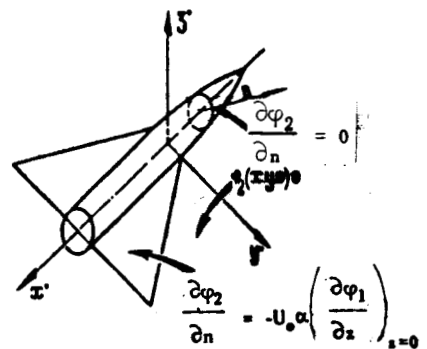


Fig.4 Boundary Conditions Defining  $\varphi_2 = \varphi - \varphi_1$ .

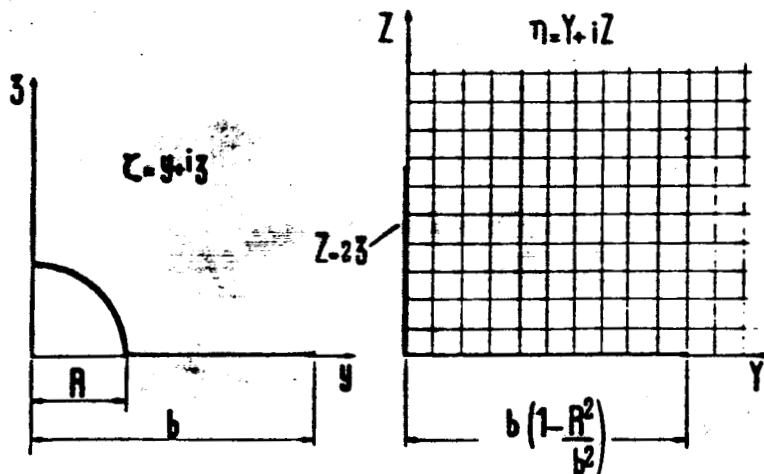


Fig.5 Introduction of the Transformed Plane  $oyz$ .

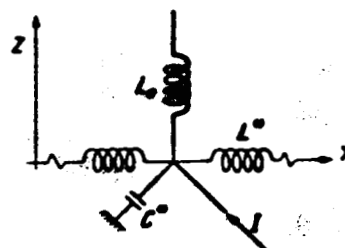


Fig.6 Boundary Conditions on the Wing.

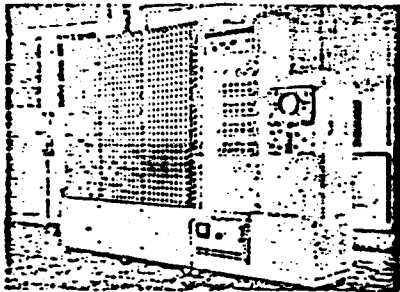


Fig.7

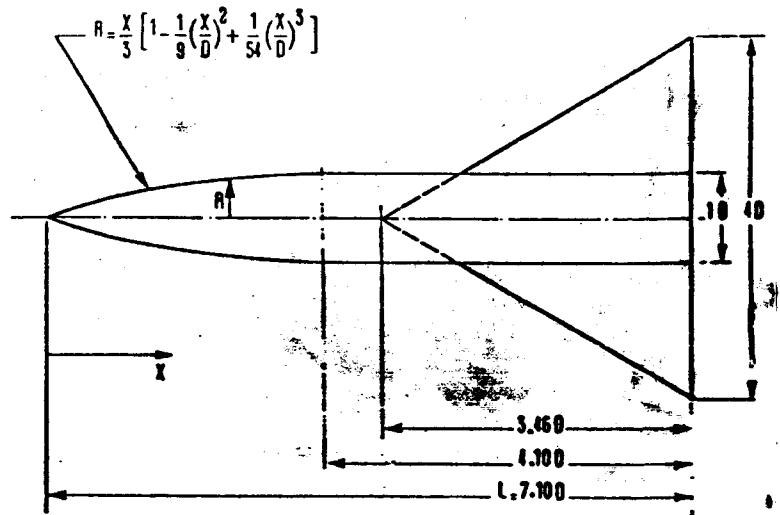


Plate 1

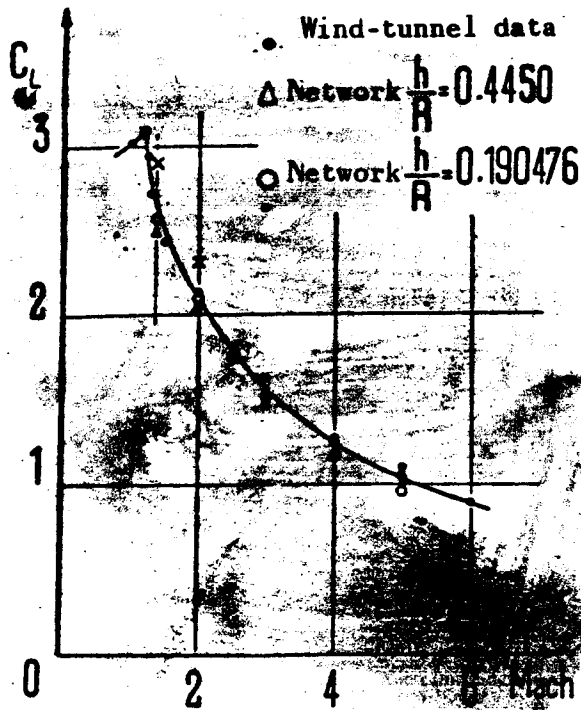


Plate 2 Coefficient of Lift.

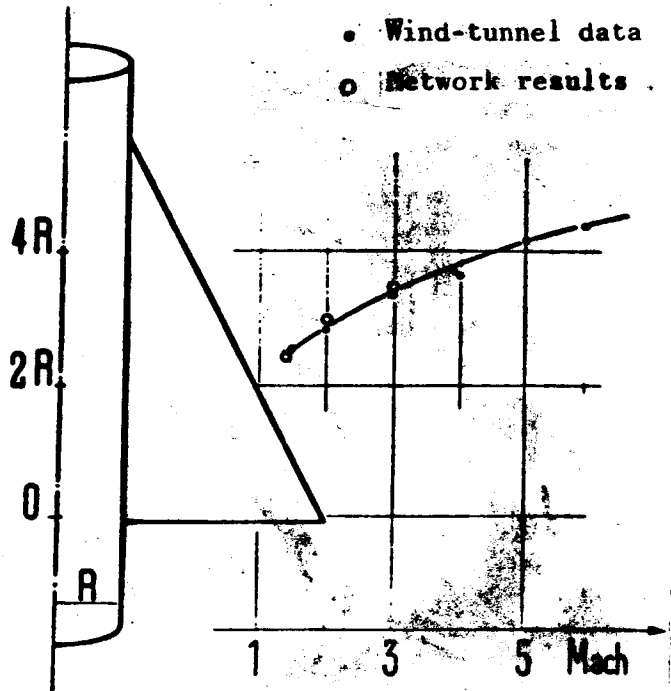


Plate 3 Position of Center of Pressure.

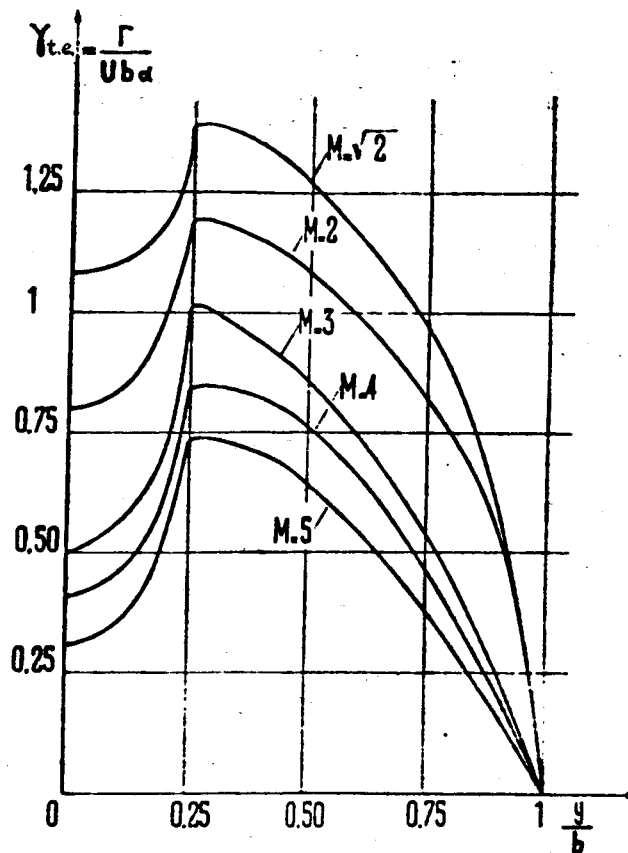


Plate 4 Distribution over Span.

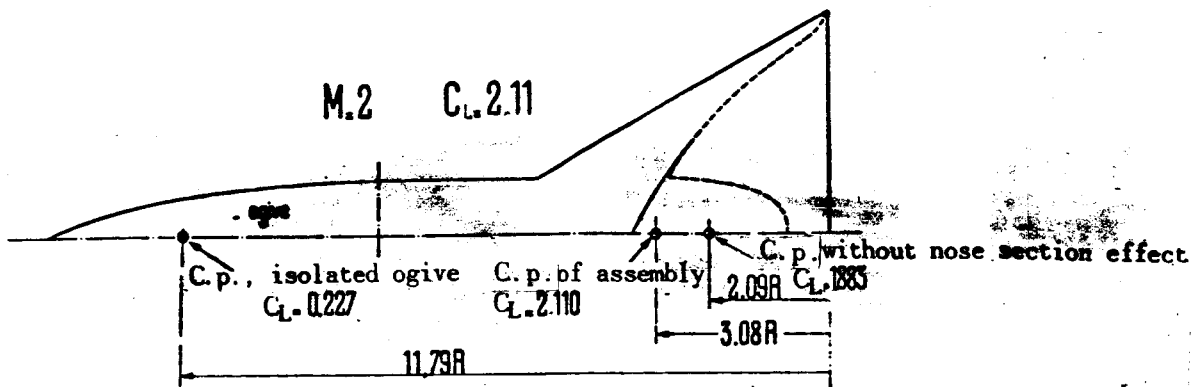


Plate 5 Location of Local Centers of Pressure and Total Center of Pressure.

Translated for the National Aeronautics and Space Administration by the O.W. Leibiger Research Laboratories, Inc.